

# Projected changes in surface solar radiation in CMIP5 global climate models and in EURO-CORDEX regional climate models for Europe

Blanka Bartók<sup>1</sup> · Martin Wild<sup>2</sup> · Doris Folini<sup>2</sup> · Daniel Lüthi<sup>2</sup> · Sven Kotlarski<sup>3</sup> · Christoph Schär<sup>2</sup> · Robert Vautard<sup>4</sup> · Sonia Jerez<sup>5</sup> · Zoltán Imecs<sup>1</sup>

Received: 28 January 2016 / Accepted: 28 November 2016 / Published online: 9 December 2016  
© Springer-Verlag Berlin Heidelberg 2016

**Abstract** The objective of the present work is to compare the projections of surface solar radiation (SSR) simulated by four regional climate models (CCLM, RCA4, WRF, ALADIN) with the respective fields of their ten driving CMIP5 global climate models. First the annual and seasonal SSR changes are examined in the regional and in the global climate models based on the RCP8.5 emission scenarios. The results show significant discrepancies between the projected SSR, the multi-model mean of RCMs indicates a decrease in SSR of  $-0.60 \text{ W/m}^2$  per decade over Europe, while the multi-model mean of the associated GCMs used to drive the RCMs gives an increase in SSR of  $+0.39 \text{ W/m}^2$  per decade for the period of 2006–2100 over Europe. At seasonal scale the largest differences appear in

spring and summer. The different signs of SSR projected changes can be interpreted as the consequence of the different behavior of cloud cover in global and regional climate models. Cloudiness shows a significant decline in GCMs with  $-0.24\%$  per decade which explains the extra income in SSR, while in case of the regional models no significant changes in cloudiness can be detected. The reduction of SSR in RCMs can be attributed to increasing atmospheric absorption in line with the increase of water vapor content. Both global and regional models overestimate SSR in absolute terms as compared to surface observations, in line with an underestimation of cloud cover. Regional models further have difficulties to adequately reproduce the observed trends in SSR over the past decades.

**Electronic supplementary material** The online version of this article (doi:10.1007/s00382-016-3471-2) contains supplementary material, which is available to authorized users.

✉ Blanka Bartók  
blanka.bartok@geografie.ubbcluj.ro

Martin Wild  
martin.wild@env.ethz.ch

Doris Folini  
doris.folini@env.ethz.ch

Daniel Lüthi  
daniel.luethi@env.ethz.ch

Sven Kotlarski  
sven.kotlarski@meteoswiss.ch

Christoph Schär  
christoph.schaer@env.ethz.ch

Robert Vautard  
robert.vautard@lscce.ipsl.fr

Sonia Jerez  
sonia.jerez@gmail.com

Zoltán Imecs  
imecs@geografie.ubbcluj.ro

<sup>1</sup> Hungarian Department of Geography, Faculty of Geography, Babes-Bolyai University, Clinicilor 5-7, Cluj-Napoca 400006, Romania

<sup>2</sup> Institute for Atmospheric and Climate Science, ETH Zurich, Universitaetstrasse 16, 8092 Zurich, Switzerland

<sup>3</sup> Federal Office of Meteorology and Climatology MeteoSwiss, Operation Center 1, 8058 Zurich-Airport, Switzerland

<sup>4</sup> Laboratoire des Sciences du Climat et de l'Environnement, IPSL, CEA/CNRS/UVSQ, Gif-sur-Yvette, France

<sup>5</sup> Department of Physics, University of Murcia, 30100 Murcia, Spain

**Keywords** Surface solar radiation · CMIP5 global climate model · EURO-CORDEX regional climate model · Cloudiness · Atmospheric absorption

## 1 Introduction

Potential future changes in the spatial and temporal distribution of surface solar radiation (SSR) not only drive environmental changes, but can also influence different sectors such as energy, hydrology or agriculture. Consecutively SSR is used as input variable in order to create comprehensive assessments of climate change impacts (Finger et al. 2012; Schewe et al. 2014; Müller and Robertson 2014; Jerez et al. 2015; Vezzoli et al. 2015). Thus the analysis of consistency regarding SSR projections among different climate models employing different parametrizations and different spatial scales is highly relevant. Quantifying the differences in SSR fields produced by different climate models indicates the degree of robustness of the projected SSR changes at different scales and gives a reference for the uncertainty transferred to impact studies.

Despite the large climate modeling community, studies addressing future projections of SSR are still scarce. A limited number of papers describe the scenarios of SSR changes based on global (Remund and Muller 2010; Crook et al. 2011; Gaetani 2014; Wild et al. 2015a) and regional (Pasicko et al. 2012; Finger et al. 2012; Panagea et al. 2014; Jerez et al. 2015) climate model simulations mainly in point of view of future solar energy applications. Focusing on Europe some controversial conclusions have been found regarding magnitude and even sign of SSR changes (Jerez et al. 2015; Wild et al. 2015a), a fact that motivated this study indeed.

In order to interpret future climate projections, an evaluation of the ability of the models to accurately simulate SSR is a crucial first step. In parallel with the continuous development of climate models the process of model evaluation has been also expanded and differences between models and observations are increasingly quantified (IPCC Climate Change 2013, Ch. 9). A comprehensive evaluation of SSR outputs from CMIP5 climate models (Taylore et al. 2012) against GEBA (Gilgen et al. 1998; Ohmura et al. 1989) and BSRN (Ohmura et al. 1998) surface observations can be found in the work of Wild et al. (2013, 2015b). The vast majority of the GCMs (38 out of the 43 models) were found to overestimate the SSR with a multi-model mean bias of  $7.4 \text{ W/m}^2$  over land. Using as reference satellite and reanalysis products, Li et al. (2013) also found an overestimation of SSR in CMIP5 models of  $2.5 \text{ W/m}^2$  globally. An overall overestimation in SSR across Europe is also reported from RCM simulations (Lara-Fangeo et al. 2012; Jerez et al. 2015). In terms of long-term variation

most of the GCMs from CMIP5 underestimate the increase (“brightening”) in SSR in cloudy and clear-sky conditions over Europe in the last decades, likely because of the inappropriate trends in aerosol atmospheric content (Ruckstuhl and Norris 2009; Allen et al. 2013; Nabat et al. 2014; Cherian et al. 2014). In general, modeling studies argue that the use of transient aerosol forcing instead of a constant one should be applied in models in order to be able to simulate regional trends in SSR (Dwyer et al. 2010; Wild and Schmucki 2011; Zubler et al. 2011b). Many efforts have been done to force the model simulations with different aerosol emission inventories (Folini and Wild 2011; Zubler et al. 2011a; Turnock et al. 2015; Chiacchio et al. 2015) in order to reproduce the solar dimming and brightening periods (Wild et al. 2005; Wild 2009) in line with observations. These studies found consistent patterns between simulated and observed SSR trends under clear-sky situations, while the effect of clouds under all-sky situations introduced substantial biases and spread among ensemble members. However, Haywood et al. (2011) conclude that while historical changes in the total SSR are likely due to aerosols effects, future changes in the clear-sky SSR may be dominated by increases in the atmospheric content of water vapor resulting from the water vapor feedback of global warming. It should be mentioned that the trends in cloud-free and all-sky surface solar radiation presented in the study are based only on the HadGEM2 global climate model simulations. Regional models are supposed to introduce added value in SSR simulations compared to GCMs as they include higher resolution stationary features, like topography and coastlines, and better representation of small-scale processes through the use of parametrization schemes (Giorgi et al. 1990; Paeth and Manning 2013; Torma et al. 2015). However at the same time, besides the biases inherited from the global models, the physical parameterizations implemented in RCMs should be also considered as potential causal factors of biases and uncertainty in RCM simulations (Jerez et al. 2013; Katragkou et al. 2015; Garcia-Diez et al. 2015). On the one hand Garcia-Diez et al. (2015) report biases in SSR with opposite sign validating WRF simulations with different model configurations, on the other hand ERA40-driven CCLM simulations underestimate SSR (Jaeger et al. 2008; Kothe et al. 2011). As reported by Kothe et al. (2011), Pessacg et al. (2014) and Garcia-Diez et al. (2015) biases of SSR in RCMs show a high dependence on cloud cover and surface albedo uncertainties.

The objective of this study is to elaborate a multi-model evaluation of SSR changes over Europe to solidly establish the state-of-knowledge in this respect and further unveil underlying causes of biases and uncertainties.

First we analyze the changes in SSR in the period of 2006–2100 projected by 4 RCMs belonging to the EURO-CORDEX framework at two different resolutions ( $0.44^\circ$

and  $0.11^\circ$ ) and also the SSR fields of ten corresponding GCMs used to drive these RCMs by providing the respective atmospheric boundary conditions, from the Coupled Model Intercomparison Project Phase five (CMIP5). Second, since significant discrepancies will be shown in the projected SSR changes in global and regional models over Europe, changes in cloud cover and other relevant quantities like atmospheric absorption, top-of-the-atmosphere (TOA) reflection and albedo are further analyzed with the aim of understanding the physical reason behind and identifying the key parameters introducing the differences. The validation of SSR and its trends over the historical period (1971–2005) is also included in the study.

The rest of the article is organized in the following way: in Sect. 2 the global and regional models considered in the study are presented and observational data are described. Section 3 contains the validation of SSR and cloud cover against ground-based observations. In Sect. 4 the main results regarding the projected SSR changes in GCMs and RCMs over Europe are detailed, furthermore projections of cloud cover and of other relevant components of the energy balance are presented in this section. Section 5 includes a wider discussion of the results and finally, in Sect. 6, the general conclusions of the study are summarized.

## 2 Data and methods

### 2.1 Model description

#### 2.1.1 CMIP5

Involving 20 climate modeling groups the Coupled Model Intercomparison Project Phase five (CMIP5) coordinates and provides global climate change experiments from more than 40 GCMs (Taylor et al. 2012). These experiments are widely used by the climate research community even for regional impact studies. Four Representative Concentration Pathways (RCPs) radiative forcing scenarios were developed: RCP2.6, RCP4.5, RCP6 and RCP8.5, where the associated numbers indicate the radiative forcing reached at the end of the 21st century compared to the preindustrial state. In the present study simulations of ten GCMs (Table 1) for RCP8.5 are considered, all of them with a single (first) ensemble member (except for EC-EARTH, where only the 12th ensemble member r12i1p1 is available). The RCP8.5 scenario was selected because the future changes in SSR are more obvious in this case, and therefore the differences between different simulations could be easier detected. This choice is considered more convenient if we would like to analyze not the evolution of future climate under different scenarios but the difference between future changes simulated by regional and global models having

the same forcing. The selection of GCMs is based on their use in the EURO-CORDEX downscaling experiment (Jacob et al. 2014). It is limited because only a few GCMs are currently downscaled to a high resolution of  $0.44^\circ$  and  $0.11^\circ$ . The daily fields of surface downwelling shortwave radiation (SSR), downwelling shortwave clear-sky radiation, upwelling surface shortwave radiation, TOA incident shortwave radiation, TOA outgoing shortwave radiation, total cloud cover, surface latent heat flux, and column water vapor are used in order to calculate seasonal and yearly means.

All GCMs include different schemes for the representation of atmospheric processes, aerosols, atmospheric chemistry, land surface, ocean processes, ocean biochemistry and sea ice. In terms of radiation, cloudiness plays a key role, which is represented differently in the various models. However significant improvements have been achieved in the last decades in terms of the climatological annual cycle of cloud amount, cloud-top pressure, and optical thickness (Klein et al. 2013).

For atmospheric aerosols, either aerosol precursor emission-driven (CanESM2, CSIRO-Mk3.6.0, HadGEM2-ES) or concentration-driven (CNRM-CM5, EC-EARTH, MPI-ESM-LR) forcing are applied depending on individual model characteristics (Table 1). Some of the models prescribe pre-computed aerosols using aerosol chemistry models (MIROC5, EC-EARTH). Models driven by aerosol concentrations incorporate aerosol inventories mainly provided by Lamarque et al. (2010). Besides of the direct effect of sulphate, black and organic carbon, sea salt, mineral dust and volcanoes, seven of the ten models (see Table 1). Include the first indirect effects of aerosols (impact of aerosol on cloud droplet radius and cloud droplet number concentration), three of them (see Table 1). Handling also the second indirect effect i.e. impact of aerosols on cloud lifetime, depth, and liquid water content.

#### 2.1.2 EURO-CORDEX

Embedded into the Coordinated Regional Climate Downscaling Experiment (CORDEX), EURO-CORDEX (Jacob et al. 2014) provides regional climate projections for Europe at grid-spacing of about 50 km ( $0.44^\circ$  resolution) and 12 km ( $0.11^\circ$  resolution). Table 2 contains the characteristics of the regional climate models considered in the study where the driving CMIP5 GCMs realizations are also listed. The RCM-simulated quantities of surface downwelling shortwave radiation, upwelling surface shortwave radiation, TOA incident shortwave radiation, TOA outgoing shortwave radiation, total cloud cover, surface latent heat flux, and column water vapor have been analyzed and compared against the corresponding outputs of the driving GCMs respectively.

**Table 1** List of GCMs considered in the study (adapted from IPCC Climate Change 2013 and Wilox et al. 2013)

Model name	Institution	Aerosol	Aerosol inventory	First/second aerosol indirect effect	Resolution [°]
CanESM2 (von Salzen et al. 2013)	Canadian Center for Climate Modelling and Analysis	Interactive	Lamarque et al. (2010)	Y/N	2.8×2.8
CNRM-CM5 (Voldoire et al. 2013)	Centre National de Recherches Meteorologiques and Centre Europeen de Recherche et Formation Avancees en Calcul Scientifique	Prescribed	Lamarque et al. (2010)	Y/N	1.4×1.4
CSIRO-Mk3.6.0 (Rotstayn et al. 2012)	Queensland Climate Change Centre of Excellence and Commonwealth Scientific and Industrial Research Organisation	Interactive	Lamarque et al. (2010) <sup>a</sup>	Y/N	1.8×1.8
EC-EARTH (Hazeleger et al. 2012)	Consortium from Europe	Prescribed	Lamarque et al. (2010)	N/N	1.13×1.12
GFDL-ESM2M (Dunne et al. 2012)	NOAA Geophysical Fluid Dynamics Laboratory	Semi-interactive	Lamarque et al. (2010)	N/N	2.5×2.0
HadGEM2-ES (Collins et al. 2011)	UK Met Office Hadley Centre	Interactive	Lamarque et al. (2010)	Y/Y	1.88×1.25
IPSL-CM5A-MR (Dufresne et al. 2012)	Institut Pierre Simon Laplace	Semi-interactive	Lamarque et al. (2010)	Y/N	2.5×1.25
MIROC5 (Watanabe et al. 2010)	University of Tokyo, National Institute for Environmental Studies, and Japan Agency for Marine-Earth Science and Technology	SPRINTARS	Lamarque et al. (2010)	Y/Y	2.8×2.8
MPI-ESM-LR	Max Planck Institute for Meteorology	Prescribed	HAC-v1 (Kinne et al. 2013)	N/N	1.88×1.87
NorESM1-M (Tjiputra et al. 2013)	Norwegian Climate Centre	CAM4-Oslo	Lamarque et al. (2010)	Y/Y	2.5×1.9

<sup>a</sup>But with black carbon increased uniformly by 25% and organic aerosol increased by 50% (Rotstayn et al. 2012)

The EURO-CORDEX platform provides various regional scale simulations using different boundary conditions. Thereby for example the difference between the projections given by one specific RCM using different forcing GCMs can be analyzed, highlighting the role of the dynamical downscaling process for radiation-related processes. For instance, CCLM simulations forced by four different GCMs (CNRM-CM5, EC-EARTH, HadGEM2-ES, MPI-ESM-LR) are available, while WRF and ALADIN are driven by a single GCM, namely IPSL-CM5A-MR and CNRM-CM5, respectively. The largest variety is provided in the case of RCA4, where ten different simulations using ten different driving GCMs (CanESM2, CNRM-CM5, CSIRO-Mk3-6-0, EC-EARTH, GFDL-ESM2M, MIROC5, NorESM1-M, HadGEM2-ES, IPSL-CM5A-MR, MPI-ESM-LR) can be accessed. However, a difficulty has been encountered in the analyses, namely that not in each case simulations at both resolution are available, e.g. CCLM simulations with different boundary forcings exist only at

0.11° resolution or RCA4 experiments with all forcings can be accessed only for the 0.44° resolution. In the present study the resolutions of the analyzed fields are given in each case.

In terms of RCM validation against observations, a strong dependence of the spatial patterns of biases regarding SSR and cloudiness on the applied convective and radiation scheme has been reported (Katragkou et al. 2015). Convection and microphysics schemes were also found to drive the difference among summer temperature biases (Vautard et al. 2013) in the EURO-CORDEX ensemble.

In terms of aerosols RCMs use different aerosol climatologies with various degrees of complexity. CCLM includes spatially variable aerosol distribution (urban/land/dust/sea-salt) derived from the old climatology of Tanré et al. (1984). This aerosol climatology has a very low resolution (T10) and strongly overestimates AOD over Europe (Zubler et al. 2011c) with unrealistic high desert dust component (Hohenegger and Vidale 2005). In RCA4

**Table 2** List of RCMs considered in the study (adapted from Kotlarski et al. 2014)

RCM (Institute) main reference	Horizontal resolution [°]	Boundary forcing	Radiation scheme	Convection scheme	Microphysics scheme	Land-surface scheme	Planetary boundary layer scheme	Aerosol climatology
CCLM 4.8.17 (Climate Limited-area Modelling-Community) <a href="http://www.cosmo-model.or">http://www.cosmo-model.or</a>	0.11	CNRM-CM5 EC-EARTH HadGEM2-ES MPI-ESM-LR ECMWF-ERAINT	Ritter and Geleyn (1992)	Tiedtke (1989)	Doms et al. (2011), Baldauf and Schulz (2004)	TERRA-ML: Doms et al. (2011)	Louis (1979)	Spatially variable aerosol distribution derived from the Tanré et al. (1984) climatology
RC4 (Swedish Meteorological and Hydrological Institute, SMHI) Samuelsson et al. (2011); Kupiainen et al. (2011)	0.44 0.11, 0.44 0.44 0.11, 0.44 0.44 0.44	CanESM2 CNRM-CM5 CSIRO-Mk3-6-0 EC-EARTH GFDL-ESM2M MIROC5 NorESM1-M HadGEM2-ES IPSL-CM5A-MR MPI-ESM-LR ECMWF-ERAINT	Savijärvi (1990), Sass et al. (1994)	Kain and Fritsch (1990, 1993)	Rasch and Kristjánsson (1998)	Samuelsson et al. (2006)	Cuxart et al. (2000)	Constant aerosol handled by the radiation scheme
WRF 3.3.1F (Institut Pierre Simon Laplace/Institut National de l'Environnement Industriel et des Risques (IPSL/INERIS)) Skamarock et al. (2008)	0.11, 0.44 0.11	IPSL-CM5A-MR ECMWF-ERAINT	RRTMG: Iacono et al. (2008)	Grell and Devenyi (2002)	Hong et al. (2004)	NOAH: Ek et al. (2003)	YSU: Hong et al. (2006)	Aerosols not considered in radiative transfer calculations
ALADIN 5.2 (Hungarian Meteorological Service) ARPEGE-Climate Version 5.2 (2011)	0.44 0.11	CNRM-CM5 ECMWF-ERAINT	Fouquart and Bonnel (1980)	Bougeault (1985)	Ricard and Royer, 1993	ISBA (Noilhan and Planton, 1989)	Troen and Mahrt (1986)	6 classes of monthly-varying aerosols: desert dust, sea salt, sulfate, black carbon, organic Tegen et al. (1997) and volcanoes

simulations aerosols are held constant through time and do not vary in space, not read explicitly, but handled by the radiation scheme. In the case of WRF 3.3.1 no representation of the aerosols can be found. Only ALADIN 5.2 incorporates a radiative scheme to take into account the direct and semi-direct effects of five aerosol types (sea salt, desert dust, sulfates, black and organic carbon aerosols) through the AOD climatology (Tegen et al. 1997) (Table 1). The spatial resolution of Tegen et al. (1997) climatology is T21, the time resolution is monthly, and in general exhibits too small AOD over most parts of Europe compared to observations (Zubler et al. 2011c). Based on Zubler et al. (2011c) calculations for the period of 1997–2003 this underestimation of aerosols led to an increase of SSR in annual mean of 10–20% south of 46°N in comparison with the climatology of Tanré et al. (1984).

The main reason of using aerosol climatology in RCM simulations instead of interactive aerosols is to reduce the calculation performance required.

## 2.2 Observational data

### 2.2.1 Solar surface radiation

The daily data of ground-based SSR are coming from the World Radiation Data Centre (WRDC, <http://wrdc.mgo.rssi.ru/>) representing the European continent by 25 stations (Table 3). The spatial distribution of the 25 WRDC stations is also presented in Online resource 3. The selection of stations is based on the data availability for the investigated period of 1971–2012. As the consequence no data for the Iberian Peninsula, France and Balkans are available. The data were recorded using standard pyranometers calibrated according to WMO standards. The yearly means considered in the validation process have been obtained by averaging the monthly means calculated as the arithmetic mean of daily sums. The data series have been homogenized using the MASH process (Szentimrey 2003). As a consequence series with physically irrelevant break points have been eliminated from the datasets, and data gaps have been filled.

### 2.2.2 Cloudiness

The synoptic visual cloudiness data are available from the “Extended Edited Cloud Report Archive” (EECRA) (Hahn and Warren 2003). In the case of validation of model outputs, 19 stations represent the European continent for the period of 1975–2005. The spatial distribution of the 19 EECRA stations is presented in Online resource 3. Similar to SSR data, cloudiness data have been independently homogenized by the MASH process. The homogenized datasets indicate stronger significant correlations between

**Table 3** List of European stations of SSR (from World Radiation Data Center) and cloud cover (Extended Edited Cloud Report Archive) observations

	Station	Latitude	Longitude	SSR (WRDC)	Clouds (EECRA)
1	ABERPORTH	52.13	−4.57	–	–
2	BERGEN	60.40	5.32	–	–
3	BRATISLAVA	48.17	17.12	–	–
4	BRINDISI	40.65	17.95	–	–
5	DEBILT	52.10	5.18	–	–
6	ESKDALEMUIR	55.32	−3.20	–	–
7	GRAZ	47.08	15.45	–	–
8	HELSINKI	60.32	24.95	–	–
9	HRADEC KRAL- OVE	50.18	15.83	–	–
10	JOKIOINEN	60.82	23.50	–	–
11	KLAGENFURT	46.65	14.33	–	–
12	KOLOBRZEG	54.18	15.58	–	–
13	LERWICK	60.13	−1.18	–	–
14	LOCARNO	46.17	8.78	–	–
15	LULEA	65.55	22.13	–	–
16	PALINURO CAPO	40.02	15.28	–	–
17	REYKJAVIK	64.13	−21.90	–	–
18	SALZBURG	47.78	13.05	–	–
19	SONNBLICK	47.05	12.95	–	–
20	STOCKHOLM	59.35	18.07	–	–
21	VALENTIA	51.93	−10.25	–	–
22	VIGNA DI VALLE	42.08	12.22	–	–
23	WARSZAWA	52.28	20.97	–	–
24	WIEN	48.25	16.35	–	–
25	ZAKOPANE	49.30	19.95	–	–

– Marks if data are available at the given station

SSR and cloudiness data than before the homogenization process.

## 3 Validation of GCMs and RCMs outputs against observations

In this section the SSR and total cloud cover historical series (1971–2005 period) from GCMs and RCMs are compared to observations. For this purpose, the nearest model grid points to the stations where observations are available (see Online resource 3) are selected and averaged, namely 25 grid points in case of SSR and 19 grid points in case of cloudiness.

Not surprisingly, the simulated SSR series show an overall overestimation compared to WRDC data (Fig. 1a) which is a known long standing problem in climate modeling

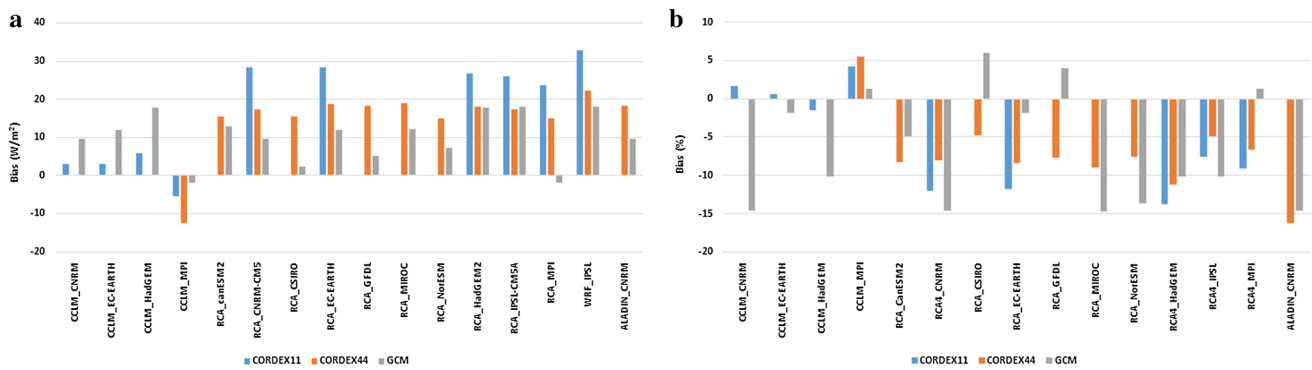


**Fig. 1** Biases in **a** SSR simulations against WRDC observations (25 stations in Europe), **b** and total cloud cover simulations against EECRA observations (19 stations in Europe). *Blue columns* depict

RCM simulations with 0.11° resolution, *orange columns* depict RCM simulations with 0.44° resolution, and *grey columns* depict simulations by the driving GCMs

(e.g. Wild et al. 1995). The lowest biases are found for the CCLM regional model, and in this case the biases of the driving GCMs are higher except for MPI. Furthermore, in the CCLM simulation driven by the MPI GCM, an underestimation of SSR is found. In case of RCA4, WRF and ALADIN, the biases in the regional models are higher than in the GCMs applied as boundary condition. Considering also the comparison between RCMs at 0.11° and 0.44° resolutions, it seems that the biases become larger with higher resolution. The multi-model bias is 9.5 W/m<sup>2</sup> for global models (average of 10 GCMs), 15.1 W/m<sup>2</sup> for RCMs at 0.44° resolution (average of 13 simulations of 4 RCMs see Table 2) and 17.2 W/m<sup>2</sup> for RCMs at 0.11° resolution (average of 10 simulations of 3 RCMs see Table 2).

Figure 1b shows the biases of simulated total cloud cover as compared to the cloud observations available from EERCA (Table 3). An overall underestimation of cloudiness is found in both GCMs and RCMs: -5.9% for GCMs, -7.3% for RCMs at 0.44° resolution and -5.5% for RCMs at 0.11° resolution. Hence, RCMs at 0.11° resolution show the lowest bias in cloud cover while the strongest overestimation of SSR, which suggests that by enhancing the representation of cloud cover at higher

resolutions larger compensating errors could be introduced in the radiation budget. Validations against satellite measurements also indicate that most GCMs tend to underestimate the amounts of low and mid-level clouds (Zhang et al. 2005).

In terms of trends, the multi-model SSR mean of the 10 GCMs reproduces the brightening in the period of 1991–2012 (Wild et al. 2005), fitting well with the observations (Table 4) in sign (however there is an underestimation of the trend by 0.92 W/m<sup>2</sup> per decade), while the “global dimming” period (1971–1990) (Stanhill and Cohen 2001) is not captured at all. In the case of the regional models a large bias can be detected between the trend in the observations and the multi-model mean, the latter indicating a continuous decrease in SSR starting from the beginning of the investigated period. However it should be mentioned that all RCMs investigated here consider temporally invariant aerosol climatologies only, therefore they cannot reproduce the full extent of the decadal SSR variability, which is considered to be mainly caused by changes in the aerosol content over Europe in the last decades (Wild 2009). In this respect, global climate models may partially be able to better reproduce SSR trends in the historical periods due to the

**Table 4** Linear trends in SSR (W/m<sup>2</sup> per decade) and total cloud cover (% per decade) over Europe in observations and in regional and global model simulations

Period	Trend of SSR (W/m <sup>2</sup> per decade)			
	WRDC (Obs)	CORDEX11	CORDEX44	GCMs
1971–2012	1.42	-0.34	-0.27	1.75
1971–1990	-1.44	-0.33	-0.21	0.73
1991–2012	3.00	-0.55	-0.30	2.08
Period	Trend of total cloud cover (% per decade)			
	EECRA (Obs)	CORDEX11	CORDEX44	GCMs
1975–2006	-0.06	-0.15	0.01	-0.32

consideration of time dependent aerosol emission or concentration changes (see Table 1).

On the other hand, the non-significant changes in total cloud cover in the period of 1975–2006 indicated by the EERCA observations is only captured by the RCMs at 0.44° resolution, whereas the GCMs and the higher 0.11° resolution EURO-CORDEX simulations give significant negative trends (Table 4).

The validation of regional climate simulations with 0.11° resolution driven by the ERA-INTERIM reanalyzes has been also elaborated in the period of 1989–2005. An overall overestimation of SSR by 17.1 W/m<sup>2</sup> has been detected which is similar with the BIAS in case of simulations driven by different GCMs (15.9 W/m<sup>2</sup>) for the same period. The smallest BIAS of −1.3 W/m<sup>2</sup> is found in the case of CCLM (+0.09 W/m<sup>2</sup> driven by GCMs, with underestimation by 7.6 W/m<sup>2</sup> in CCLM simulations driven by MPI), and an overestimation of solar surface radiation by 19.5 W/m<sup>2</sup> in ALADIN, by 20.6 W/m<sup>2</sup> in RCA4 and by 29.4 W/m<sup>2</sup> in WRF. These BIAS in the simulations driven by GCMs are 19.1 W/m<sup>2</sup> (with 0.44° resolution), 25.2 and 32.1 W/m<sup>2</sup>, respectively. In terms of trends (compared to the observations, 2.28 W/m<sup>2</sup> per decade) a stronger trend is detected in the case of ALADIN simulations (3.59 W/m<sup>2</sup> per decade), weaker trend in CCLM (0.23 W/m<sup>2</sup> per decade) and RCA4 (0.69 W/m<sup>2</sup> per decade) and opposite trend in WRF (−0.84 W/m<sup>2</sup> per decade). In simulations forced by different GCMs these trends are 4.97 W/m<sup>2</sup> per decade in ALADIN, 0.10 W/m<sup>2</sup> per decade CCLM, −0.17 W/m<sup>2</sup> per decade in RCA4 and −0.53 W/m<sup>2</sup> per decade in WRF.

In addition to prevailing large-scale conditions the nested regional climate models are constructed to describe small-scale atmospheric features such as convective cell, orography, costal line, land cover all having influence on the local climate. A large number of studies are assessing the added value of regional climate models (Xie et al. 2015; Di Luca et al. 2015) comparing them with observations. In general the modelling community agree that regional models can add value, however it highly depends on the variable of interest and the location (Feser et al. 2011). In our study the validation of SSR fields coming from GCMs forced regional climate models indicates similar BIAS as in the case of validation of hindcast simulations (the largest difference of BIAS from individual validations is 7.1 W/m<sup>2</sup>) which confirms the fact that radiation processes in RCMs are not significantly affected by the physical processes constrained by boundary conditions. This could imply that the inconsistencies between the SSR simulations of GCMs and RCMs, and also the BIAS are mainly dominated by the parameterization of local processes and by the compensating errors resulting from this parameterizations. These errors, however, cannot be identified from a single output, their identification requires the examination of individual

physical processes in the simulation not included in the present study. Regarding the validation of long term SSR trends the observational records showed a strong dependency to atmospheric aerosol content in the last decades over Europe (Wild 2009), hereafter because of the lack of time varying aerosol input the RCMs are not able to reproduce these changes. On the other hand mainly in midlatitudes the internal variability (not analysed in the study) plays a dominant role in multidecadal atmospheric circulation changes which becomes higher at finer spatial and temporal scales shaping regional climate patterns (Maraun et al. 2010). This can also influence the ability of regional climate models to reproduce trends.

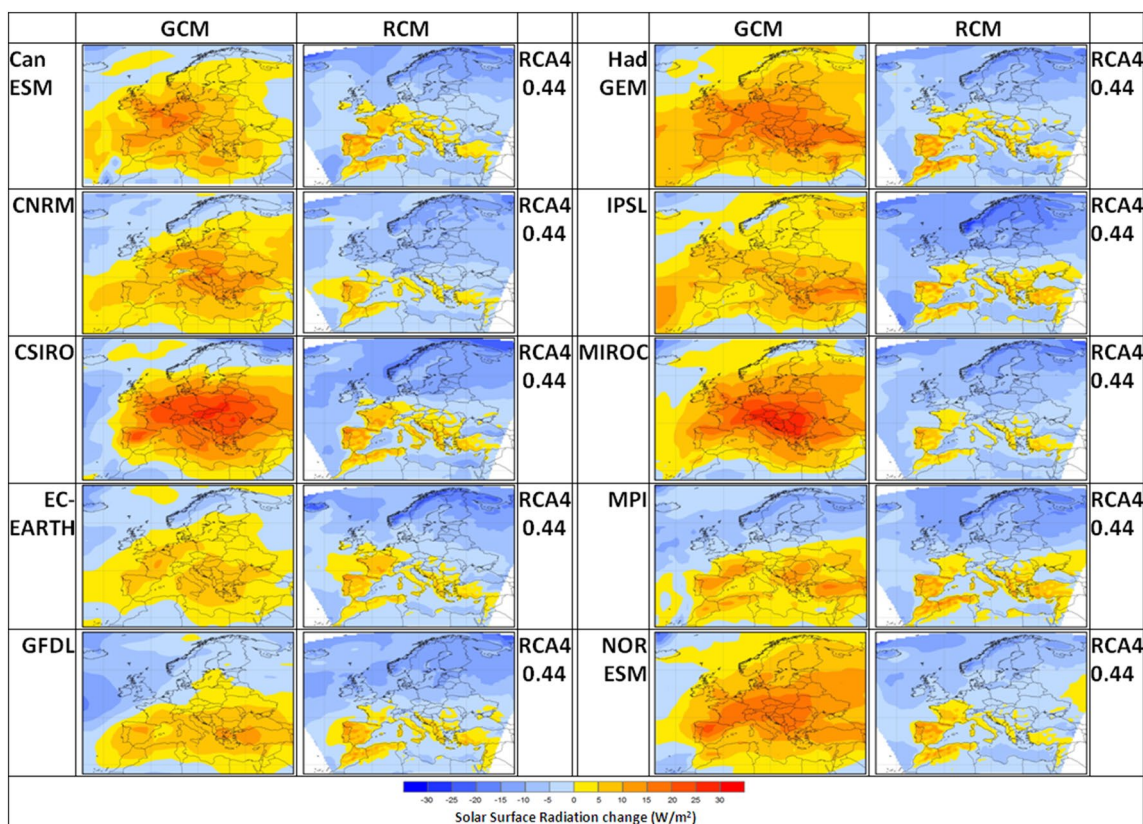
## 4 Climate change scenarios

### 4.1 Annual changes in SSR from GCMs and RCMs

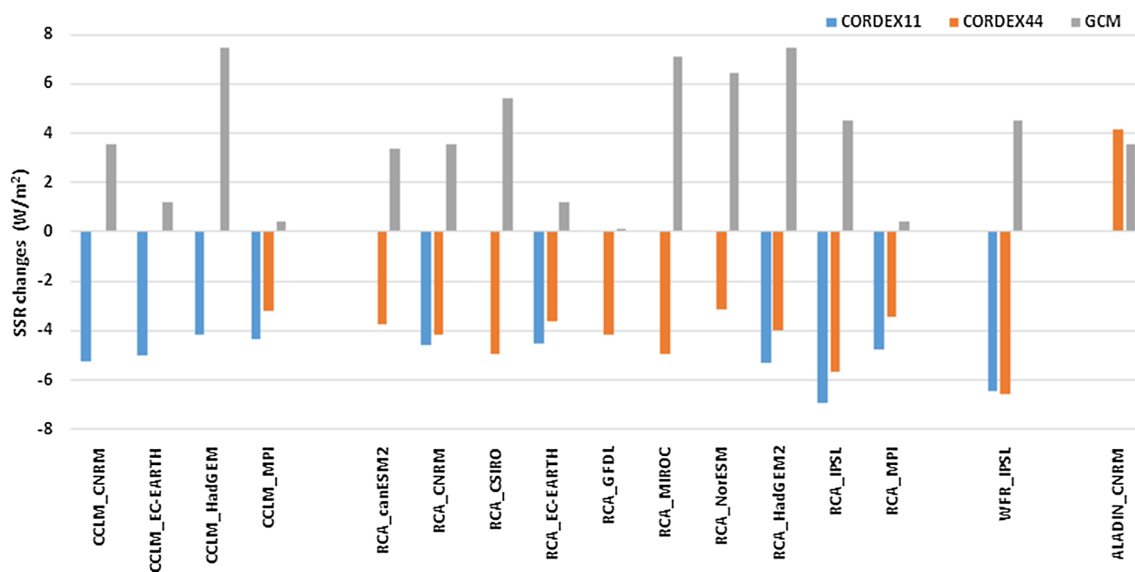
In this section future projections of SSR based on regional and global climate model simulations are assessed.

Figure 2 shows the changes of SSR for the case of the RCA4 regional model (at 0.44° resolution) with ten different GCMs (whose SSR projections are also shown in Fig. 2) applied as boundary forcing. The changes are given in absolute values (W/m<sup>2</sup>) defined as the difference between the future projections under RCP8.5 (2071–2100) and the historical simulation (1971–2005). The forcing GCMs indicate an overall increase in SSR over the European domain (27 N–72 N, 22 W–45E) to the end of the century, the multi-model mean projection being 3.96 W/m<sup>2</sup>, with the individual signals exceeding even 20 W/m<sup>2</sup> in some places. Strong positive changes are mainly located in the center part of the continent (CSIRO, HadGEM, MIROC, NorESM) except for the MPI and GFDL models that only project an increase in SSR over the southern part of the domain, with their signals being negative in the central and northern parts.

Contrary to the GCM projections, the projections of RCA4 using different boundary conditions give on average (over all realizations and the entire European domain) a general decrease in SSR by 4.18 W/m<sup>2</sup> to the end of the century. The absolute difference between the SSR multi-model changes projected by the 10 GCMs and by the 10 realizations of RCA4 presented in Fig. 2 is 8.14 W/m<sup>2</sup>, including a change of sign. It is also noteworthy that both the pattern of SSR changes and the mean change over the domain seem to be very similar in all realizations of RCA4, despite much stronger differences both in magnitude and pattern in the GCM ensemble. Obviously, the SSR changes in the RCM are mainly controlled by internal processes of the RCM and little influenced by the boundary forcing applied.



**Fig. 2** Annual projected changes in SSR in the RCA4 regional model and in different driving GCMs. The changes are defined as the difference between the future projections for RCP8.5 (2071–2100) and the historical simulation (1971–2005)



**Fig. 3** Annual changes in SSR in individual RCMs (first name on x axes) and in GCM applied as boundary conditions (second name on x axes) over the European domain. *Blue columns* depict changes for RCMs with 0.11° resolution, *orange columns* depict changes for

RCMs with 0.44° resolution, and *grey columns* depict changes in GCMs. The changes are defined as the difference between the future projections of RCP8.5 (2071–2100) and historical simulation (1971–2005)

Considering realizations of CCLM with  $0.11^\circ$  resolution (Fig. 3, Online Resource 1) the absolute difference between the SSR changes in RCMs and in the 4 driving GCMs is  $7.85 \text{ W/m}^2$ ,  $-4.69 \text{ W/m}^2$  and  $+3.16 \text{ W/m}^2$  respectively. In WRF simulations the SSR changes are  $-6.42 \text{ W/m}^2$  (with  $0.11^\circ$  resolution) and  $-6.57 \text{ W/m}^2$  (with  $0.44^\circ$  resolution) while the driving GCM (IPSL) gives an increase in SSR of  $4.53 \text{ W/m}^2$  (Fig. 3, Online Resource 1).

In most cases the opposite sign in SSR changes between an RCM and its driving GCM is evident except for ALADIN driven by CNRM-CM5. In the case of ALADIN, an increase in SSR of  $4.14 \text{ W/m}^2$  is projected for Europe, which is stronger than the changes projected by the driving GCM ( $3.52 \text{ W/m}^2$ ). It should be mentioned that the regional model of ALADIN and its driving GCM, namely CNRM-CM5, have the same physical parameterizations contrary to the other simulations. On the other hand the ALADIN model implies the Tegen climatology which underestimates the AOD over Europe (see Sect. 2.1.2). These facts reinforce the idea that the trends in SSR simulated by RCMs depend more on physical parameterizations of the inner model than on the lateral boundary conditions.

Opposite trends in the future projections of SSR between RCMs (only at  $0.11^\circ$  resolution) and respective GCMs can also be seen in Fig. 4. The anomaly time series in Fig. 4 are made up from the average over the 25 grid cells where the 25 WRDC observational sites (Table 3) are located. The multi-model mean of the five GCMs (Fig. 4a) shows an increase in SSR with a rate of  $0.17 \text{ W/m}^2$  per decade for the period of 2006–2100, while this change in the multi-model mean of the 3 RCMs (Fig. 4b) is  $-0.72 \text{ W/m}^2$  per decade considering the  $0.11^\circ$  resolution realizations and  $-0.47 \text{ W/m}^2$  per decade considering the  $0.44^\circ$  resolution realizations (not shown on Fig. 4b).

The differences detected in SSR changes between GCMs and RCMs evidence the fact that even if the boundary

conditions regarding meteorological parameters are taken from GCMs, the processes affecting radiation are represented differently in global and regional models. The differences can originate from the different radiation schemes applied in GCMs and RCMs but also from changing the parametrization of other processes affecting radiation like cloudiness. These changes strongly influence the whole radiation balance potentially introducing compensating errors which could reduce the ability of the climate models to simulate the right amounts of radiation in the shortwave and longwave spectrum (Klein et al. 2013).

Another aspect in understanding the difference between RCMs simulations, however, is the internal variability of the regional models (Giorgi and Gutowski 2015). Besides the fact that RCMs are constrained by lateral boundary conditions, recent studies have argued that even on decadal or multidecadal scale RCMs also exhibit internal variability, namely could produce different experiments for the same set of lateral conditions (Bellprat et al. 2012; Lucas-Picher et al. 2008). Internal variability might vary as a function of season showing larger differences in summer over midlatitudes (Caya and Biner 2004; Giorgi and Bi 2000), as a function of domains size where differences increase as the size of the domain getting larger (Vannitsem and Chome 2005) and as a function of geographical location (Alexandru et al. 2007). The spatial patterns of positive and negative changes are similar in all RCMs (Online Resource 1) except for ALADIN. Regardless of the boundary conditions three out of the four RCMs indicate a SSR increase in the southern part of the continent (Iberian Peninsula, France, Italy, Balkan Peninsula, Turkey and northern edge of Africa) and a decrease in SSR in the other parts of the domain. Also in the regional models a sharp difference between sea and land surfaces can be detected (see e.g. Iberian Peninsula). It can be concluded that the regional model simulations

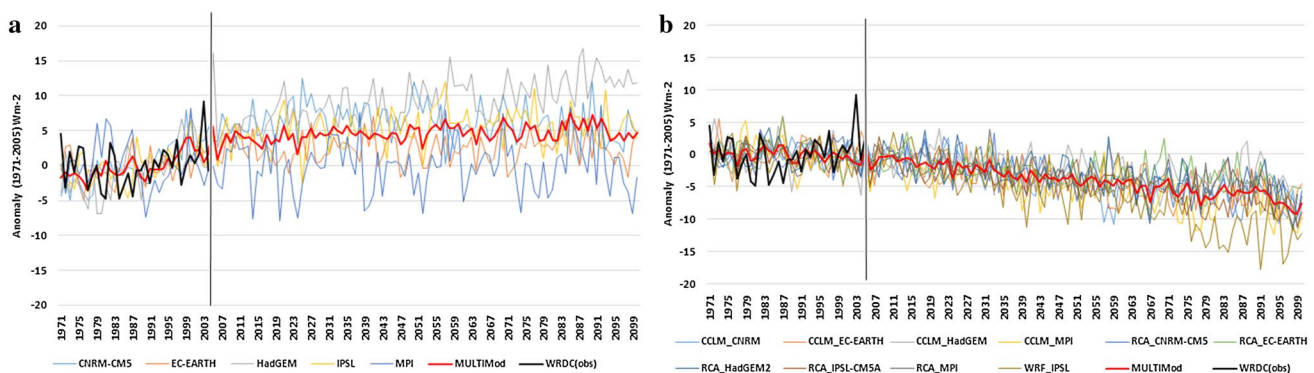
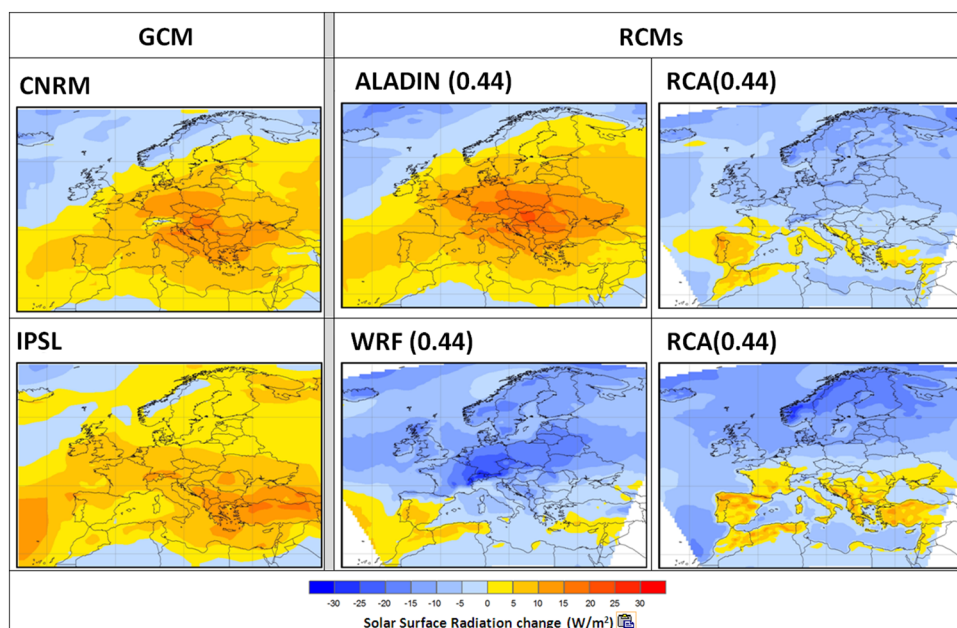


**Fig. 4** Annual changes (anomaly from 1971 to 2005) in SSR in GCMs (a) and RCMs (b), red curve—multimodel mean, black curve—observations (in legend of b first is the name of the RCM, second is

the name of the driving GCM). The anomaly time series are made up from the average over the 25 grid cells where the 25 WRDC observational sites (Table 3) are located

**Fig. 5** Annual changes in SSR in different RCMs driven by the same GCM. The changes are defined as the difference between the future projections of RCP8.5 (2071–2100) and the historical simulation (1971–2005)



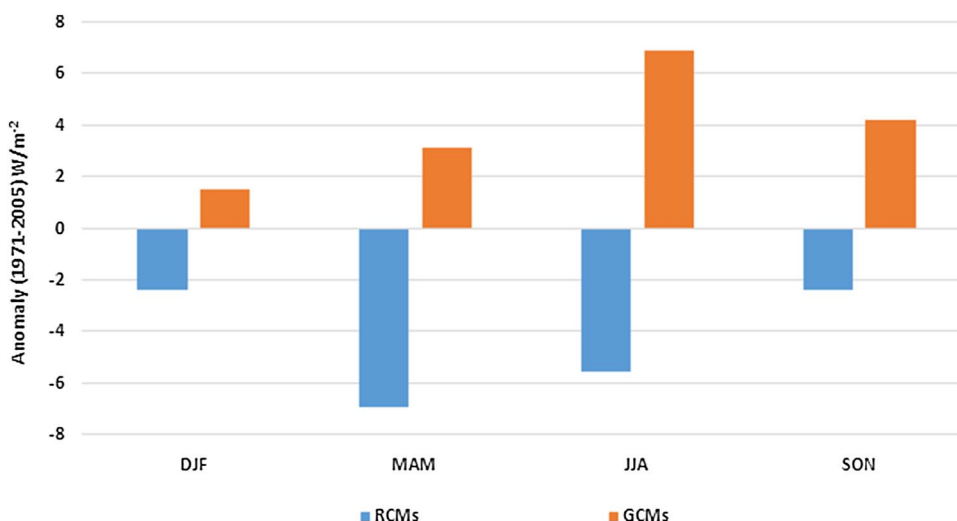
regarding SSR are not sensitive to the boundary conditions coming from different GCMs (Fig. 2 and also Online Resource 1). The same conclusion can be drawn if we analyze different RCM outputs having the same GCM forcing as shown in Fig. 5. In these examples both global climate models (CNRM and IPSL) indicate a robust increase over Europe. In the first case, the ALADIN regional model gives an even stronger increase in SSR than the driving GCM, while RCA4 gives changes with opposite sign except for the Iberian Peninsula. In the second case, in contrast to the driving GCM, both regional models, namely WRF and RCA4, project a decrease in SSR, although with different spatial distributions (the first one projects stronger SSR decrease in the center part

of the continent and the second one in the northern part of the continent).

#### 4.2 Seasonal changes in SSR from GCMs and RCMs

The opposite sign of SSR projections between GCM and RCM simulations presented in Figs. 3 and 4 can also be detected at seasonal scale (Fig. 6 and Online Resource 2) over the whole European domain. The multi-model mean of the 10 GCMs included in the study gives SSR changes (2071–2099 vs. 1971–2005) of 1.5 W/m<sup>2</sup> (1.9%) in DJF, 3.1 W/m<sup>2</sup> (1.5%) in MAM, 6.9 W/m<sup>2</sup> (2.6%) in JJA and 4.2 W/m<sup>2</sup> (3.3%) in SON (Fig. 6). In the case of the multi-model mean of the four RCMs (including 0.11° and 0.44° resolution) changes are -2.3 W/m<sup>2</sup> (-3.0%), -6.8 W/m<sup>2</sup>

**Fig. 6** Seasonal changes in SSR in the 4 regional models including realizations at 0.11° and 0.44° (blue columns) and in 10 global climate models (orange columns) used as boundary condition over the European domain. The multimodel changes are defined as the difference between the future projections of RCP8.5 (2071–2100) and the historical simulation (1971–2005)



(−3.3%), −5.5 W/m<sup>2</sup> (−2.2%) and −2.3 W/m<sup>2</sup> (−1.9%) respectively. Similar to the yearly changes, the regional models give decreasing trends in each season excepting ALADIN simulations (changes for individual models are presented in Online Resource 4). Generally, the largest positive SSR changes in the GCMs are taking place during summer and autumn while in the case of the RCMs largest negative changes occur in spring and summer. In general the spatial patterns of SSR changes in GCMs and RCMs differ during spring, summer and autumn, but fairly similar spatial distributions are obtained for wintertime (Online Resource 2). The physical background to understand the differences between the seasonal changes is partially explained in the discussion.

### 4.3 Changes in cloudiness

Cloudiness can be considered as the main local modulator of SSR (Garcia-Diez et al. 2015; Kothe et al. 2011). In the present study future changes in cloudiness have been examined in order to verify if the behavior of cloudiness in model simulations is consistent with the reported differences in SSR changes. Figure 7a presents the evolution (anomalies with respect to the 1971–2005 climatology) in the total cloud fraction averaged over the 19 grid cells collocated with the observational sites (see Table 3) from 5 GCMs and Fig. 7b the results from 2 RCMs (with 0.11° resolution) that were driven by these 5 GCMs. In the GCMs the multi-model mean shows a decrease in cloudiness of −0.26% per decade (significant trend at  $p=0.05$ ) for the period of 2006–2100, which is in line with the increase in SSR presented in Fig. 4a. Surprisingly the changes in total cloud fraction in the case of the regional models is −0.01% per decade for the period of 2006–2100, which is non-significant at  $p=0.05$ . Consequently, the detected significant decrease in SSR (Fig. 4b) cannot be entirely explained by

the behavior of cloudiness. Therefore, the next Section addresses further research on that.

### 4.4 Atmospheric absorption and TOA reflection

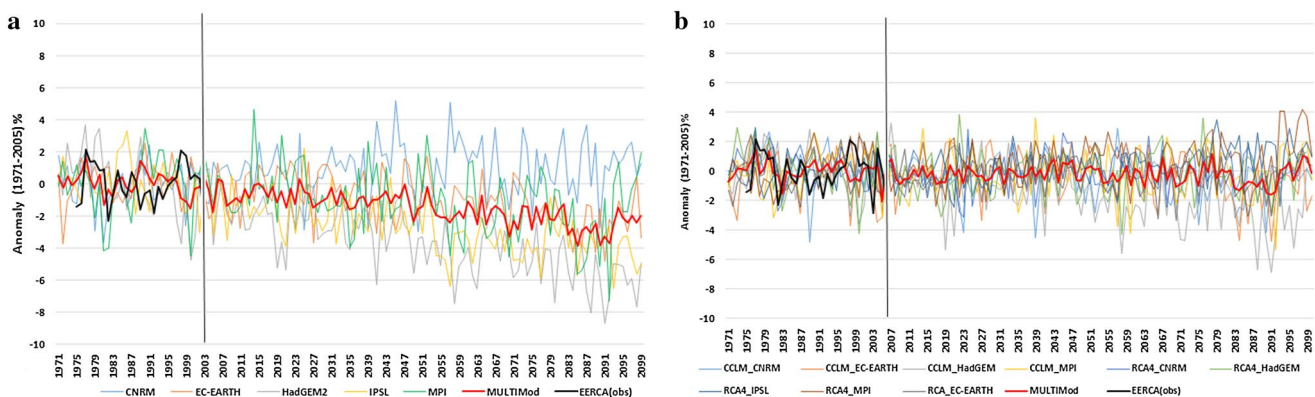
Going one step further, long-term changes in atmospheric absorption and top-of atmosphere (TOA) reflection have been investigated. These magnitudes are calculated using Eqs. (1) and (2):

$$ASR_{\text{atm}} = TOA_{\text{net}} - ASR_{\text{surf}} \quad (1)$$

$$ASR_{\text{surf}} = (1 - \alpha) SSR \quad (2)$$

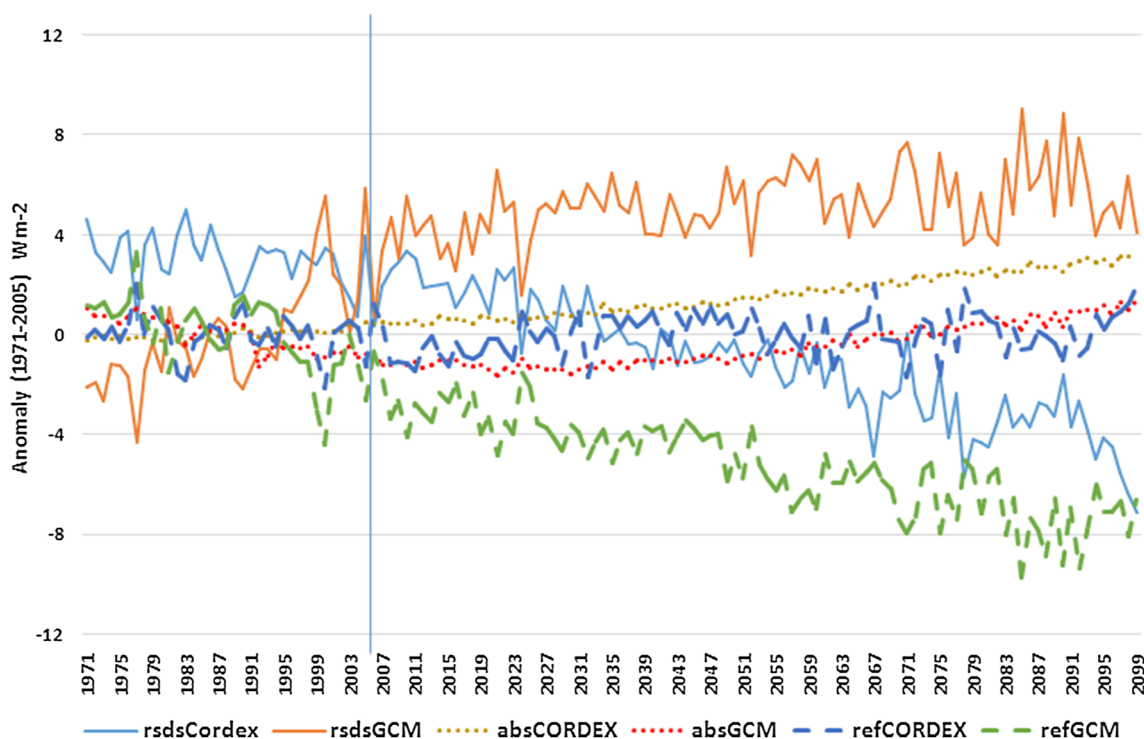
where  $ASR_{\text{atm}}$  denotes atmospheric absorption,  $TOA_{\text{net}}$  denotes net shortwave radiative flux through the top of atmosphere,  $ASR_{\text{surf}}$  is the absorption at the surface, and  $\alpha$  is the surface albedo.

Figure 8 depicts the evolution of the anomalies of SSR, atmospheric absorption and TOA reflection (reference period is 1971–2005) in 3 RCMs with 0.11° resolution (CCLM, RCA4 and WRF) and in the GCMs applied as boundary condition (CNRM, MPI, HadGEM and IPSL). The curves represent the mean changes averaged over the 25 grid cells where the WRDC observational stations are located. The multi-model mean of GCMs indicates a decline of TOA reflection of −0.60 W/m<sup>2</sup> per decade in the period of 2006–2100, which is in line with the decrease in cloudiness, see Fig. 7a. Atmospheric absorption shows an increase of 0.28 W/m<sup>2</sup> per decade until the end of the century, limiting the increase in SSR which shows a trend of +0.22 W/m<sup>2</sup> per decade (in case of the four GCM considered here). In the case of RCMs the TOA reflection shows no significant changes while the increase in atmospheric absorption of 0.31 W/m<sup>2</sup> per decade contributes to the attenuation of the surface solar radiation that exhibits a trend of −0.72 W/m<sup>2</sup> per decade.



**Fig. 7** Annual changes (anomaly from 1971 to 2005) in total cloud fraction in GCMs (a) and RCMs (b), red curve—multimodel mean, black curve—observations. The anomaly time series are made up

from the average over the 19 grid cells where the 19 EECRA observational sites (Table 3) are located



**Fig. 8** Annual changes (multimodel means) in SSR, atmospheric absorption and TOA reflection in GCMs and RCMs (the anomaly time series are made up from the average over the 25 grid cells where the 25 WRDC observational sites in Table 3 are located)

### 5 Discussion

One main question that remains to be addressed is why the changes in cloudiness are projected differently in global and regional models. Even through the parametrization is differing from one model to another, a general conclusion can be drawn regarding the consistency of changes. In the GCMs cloudiness shows an overall decline but the spread between single models is larger (the range between maximum and minimum anomalies is 15.3% of the absolute cloud cover). The multi-model mean of trends in total cloud fraction in RCMs has no significant trend and the spread between individual realizations is smaller (the range between maximum and minimum anomalies is 10.9% of the absolute cloud cover). In the GCMs there is an overall decrease in cloudiness over the entire domain (although mainly over land surfaces), while in the RCMs the changes are not so uniformly distributed, and local patterns can be detected (see Online Resource 1). In particular, a sharp contrast is shown in RCMs between ocean and land surfaces, with an overall increase in cloudiness and decrease in SSR in the North Atlantic region, and a significant decrease in cloudiness and increase in SSR over the land surfaces south to the 50 N latitude (e.g. see Iberian Peninsula in Online Resource 1). These spatial patterns of cloud cover changes, and consequently changes in SSR, are similar in

three RCMs, namely in CCLM, RCA4 and WRF (excluding ALADIN), but cannot be clearly detected in the GCMs.

The spatial difference in SSR changes between RCMs and GCMs is present mainly in the warm period of the year (spring and summer). In this period the amount of cloudiness is strongly related to the convection. Analyzing precipitation fields Turco et al. (2013) also reported inconsistent projections from the same GCM driving different RCMs.

Strongly linked to atmospheric circulation the quality of RCMs also depends on the sea surface conditions determined by the forcing GCMs (Rummukainen 2010). The advantage of a coupled regional ocean model, not the case in EURO-CORDEX simulations, is to provide sea surface temperature and sea ice extend fields with higher resolution compared to the limited one of the ocean model component of GCMs. This kind of improvement is mostly required in coastline regions with complex sea-land-atmosphere interactions. Focusing on the North Sea and Baltic Sea region Tian et al. (2013) in their work demonstrated that coupled fine-grid ocean model within RCMs is useful not only to study local climates but also to prevent sea surface temperature biases (especially in winter season) in the feedback process.

At regional scale evapotranspiration plays a key role in providing sufficient water vapour for convective cloud formation. The intensity of evapotranspiration however

is correlated to the soil moisture in terms of water limitation (Seneviratne et al. 2010; Jerez et al. 2012; Wild et al. 1996). Some studies have argued that during summertime GCMs tend to dry out (Wild et al. 1996, 1997) over Europe (or midlatitude continents) so that hardly any humidity for cloud formation is available. This phenomenon can also be detected in the latent heat flux changes in the case of the GCMs considered here, where a decline of  $0.54 \text{ W/m}^2$  per decade under the RCP8.5 scenario is found over Europe (Fig. 9a) in the period of 2006–2100. However a strong decrease of  $-0.82 \text{ W/m}^2$  per decade is detected in the second part of the period (after 2050), while in the first part of the period the change is  $-0.3 \text{ W/m}^2$  per decade, suggesting an intensified drying towards the end of the century. At the same time RCMs provide sufficient humidity for convective cloud formation according to the increase in latent heat flux in the RCM multi-model mean with  $0.76 \text{ W/m}^2$  per decade in the projected period of 2006–2100 (Fig. 9b). Therefore in this case the amount of humidity in RCMs does not constitute a limiting factor for convective cloud formation,

which may explain why the total amount of cloudiness in the regional models is not declining.

In order to confirm the results in Sect. 3.4, the simulated changes in water vapour have been checked. Figure 10a shows the changes in absolute values of column water vapour ( $\text{kg/m}^2$ ) in nine GCMs, and Fig. 10b depicts the changes in two RCMs (with  $0.11^\circ$  resolution). In both cases an increase in water vapour can be detected ( $0.53 \text{ kg/m}^2$  per decades in GCMs and  $0.52 \text{ kg/m}^2$  per decades in RCMs in the period of 2006–2100), which is in line with the detected increase of atmospheric absorption.

Besides cloudiness, the connection between SSR changes and the way in which aerosols are handled by the models have been assessed. Grouping the GCMs into categories of models with interactive aerosols (CanESM2, CSIRO-Mk3.6.0, HadGEM2-ES), models with semi-interactive aerosols (GFDL-ESM2M, IPSL-CM5A-MR), and models with prescribed (but time varying) aerosols (CNRM-CM5, EC-EARTH, MPI-ESM-LR) a larger spread of SSR changes can be detected in case of models with interactive aerosols ( $27.4 \text{ W/m}^2$ ). In the case of models

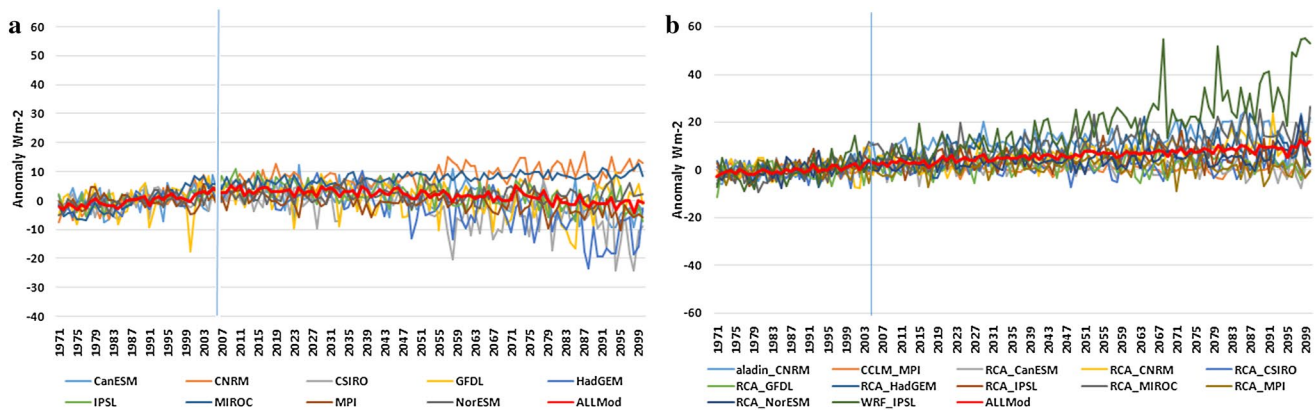


**Fig. 9** Annual changes (anomaly from 1971 to 2005) in latent heat flux in GCMs (a) and RCMs (b), red curve—multimodel mean (the anomaly time series are made up from the average over the 25 grid cells where the 25 WRDC observational sites in Table 3 are located)

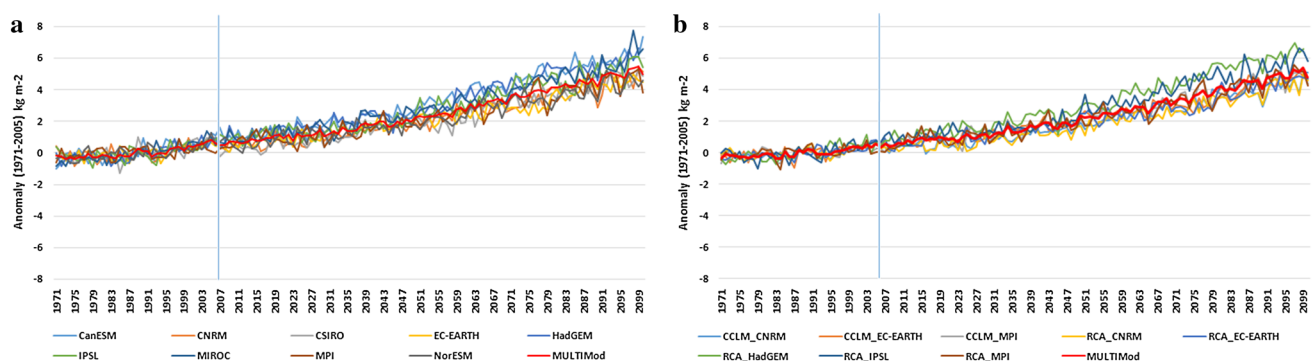


**Fig. 10** Annual changes (anomaly from 1971 to 2005) in column water vapor in GCMs (a) and RCMs (b), red curve—multimodel mean (the time series are made up from the average over the 25 grid cells where the 25 WRDC observational sites in Table 3 are located)

with semi-interactive aerosols the range of SSR changes is  $18.7 \text{ W/m}^2$ , while in the case of models having prescribed aerosols this range is  $20.4 \text{ W/m}^2$ . The larger spread in SSR changes projected by the models with interactive aerosols has been also found in the present assessment including 36 CMIP5 GCMs. At the same time all RCMs considered in this study include prescribed (time invariant) aerosol inventories. Therefore, the different way of handling aerosols can additionally explain the fact that the spread of projected changes of SSR are larger in GCMs and more consistent in RCMs.

## 6 Conclusion

The components of the shortwave radiation budget constitute key parameters in climate modeling. However there are very few studies on the evaluation of these quantities as they are simulated by different climate models both for future and present periods respectively, especially regarding solar surface radiation (SSR).

In the present study model-projected future changes in SSR over Europe have been assessed. Four RCMs and their ten driving GCMs have been considered and a remarkable discrepancy between global and regional model projections has been detected. Global climate models indicate a sustained increase in SSR over the European domain along the period 2004–2100 under the RCP85 scenario, while a general decrease in SSR has been detected in three out of the four regional models (CCLM, RCA4 and WRF). Significant decrease of SSR in case of CCLM has also been reported by Kothe et al. (2011), which is the consequence of the robust overestimation of aerosols in the Tanré et al. (1984) climatology used in these simulations (Zubler et al. 2011c). The fourth regional model, namely ALADIN5.2, was the only indicating increase of SSR. The opposite evaluation of SSR in the ALADIN model partially could be explained on the one hand by the fact that only ALADIN introduces direct and semi-direct effects of five aerosol types. On the other hand the Tegen et al. (1997) climatology used in these simulations underestimates the aerosols over the continent thus introduces higher SSR also reported in the work of Zubler et al. (2011c). Consequently the quality of aerosol information introduced in regional climate models has a significant impact on the BIAS of SSR simulations, however, their improvements do not always lead to general BIAS reducing because the compensating errors after model tuning. Overall the projected SSR changes are similar among the CCLM, RCA4 and WRF simulations irrespective of the boundary conditions taken from different GCMs. It can be argued that RCMs take boundary conditions from GCMs only for temperature, pressure, wind

humidity, sea surface temperature and sea ice extend, while the radiation scheme, the microphysics scheme and the convective cloud scheme is running fairly independently in each case. This fact is also confirmed by comparing the RCMs validations with ones of hindcast simulations.

The opposite sign of SSR changes in the regional and global models is attributed mainly to the different behaviour of the simulated cloud cover. In the global models cloudiness shows a significant decrease over Europe and, despite the fact that the atmospheric absorption is increasing due to increased water vapour there is still a surplus of energy at the surface as indicated by the positive trends in SSR. In RCMs no significant changes in cloud cover can be detected, thus the total cloud amount changes are not expected to induce changes in SSR. At the same time, regional models simulate an increase in atmospheric absorption (with similar magnitude as in GCMs), which, unlike in the GCMs, is not compensated by the increase in SSR due to the less cloudiness, finally causing a decrease in SSR.

The results of the study highlight the importance of evaluating the SSR future projections coming from different type of climate models and the detected discrepancies should be taken into account also in the interpretations of SSR based impact studies.

**Acknowledgements** The first author thanks for the Scientific Exchange Programme NMS-CH, for supporting by SCIEX postdoctoral fellowship (No. 13.155-2) and for the Young Research Grant supported by Babes-Bolyai University (No. GTC-31779/2016). The study also received support from the CEA-DSM CLLIMIX project.

## References

- Alexandru A, de Elia R, Laprise R (2007) Internal variability in regional climate downscaling at the seasonal scale. *Mon Weather Rev* 135(9):3221–3238
- Allen RJ, Norris JR, Wild M (2013) Evaluation of multidecadal variability in CMIP5 surface solar radiation and inferred underestimation of aerosol direct effects over Europe, China, Japan, and India. *J Geophys Res* 118:6311–6336
- ARPEGE-Climate Version 5.2 (2011). <http://www.cnrm-game-meteo.fr/gmgec/arpege-climat/ARPLI-V5.2/doca/arp52ca.pdf>. Accessed 30 Sept 2016
- Baldauf M, Schulz JP (2004) Prognostic precipitation in the Lokal-Modell (LM) of DWD. *COSMO. Newslett* 4:177–180
- Bellprat O, Kotlarski S, Lüthi D, Schär C (2012) Exploring perturbed physics ensembles in a regional climate model. *J Climate* 25:4582–4599
- Bougeault P (1985) A simple parameterisation of the large-scale effects of cumulus convection. *Mon Wea Rev* 113:2108–2121
- Caya D, Biner S (2004) Internal variability of RCM simulations over an annual cycle. *Clim Dyn* 22:33–46
- Cherian R, Quaas J, Salzmann M, Wild M (2014) Pollution trends over Europe constrain global aerosol forcing as simulated by climate models. *Geophys Res Lett* 41:2176–2181. doi:10.1002/2013GL058715

- Chiacchio M, Solmon F, Giorgi F, Stackhouse P, Wild M (2015) Evaluation of the radiation budget with a regional climate model over Europe and inspection of dimming and brightening. *J Geophys Res* 120:1951–1971. doi:[10.1002/2014JD022497](https://doi.org/10.1002/2014JD022497)
- Collins WJ et al (2011) Development and evaluation of an Earth-System model- HadGEM2. *Geosci Model Dev* 4:1051–1075
- Crook JA, Jones LA, Forster PM, Crook (2011) Climate change impacts on future photovoltaic and concentrated solar power energy output. *Energy. Environ Sci* 4(9):3101–3109
- Cuxart J, Bougeault P, Redelsperger JL (2000) A turbulence scheme allowing for mesoscale and large-eddy simulations. *Q J R Meteorol Soc* 126:1–30
- Di Luca A, de Elía R, Laprise R (2015) Challenges in the quest for added value of regional climate dynamical downscaling. *Curr Clim Change Rep* 1:10–21. doi:[10.1007/s40641-015-0003-9](https://doi.org/10.1007/s40641-015-0003-9)
- Doms G, Förstner J, Heise E, Herzog HJ, Raschendorfer M, Schrodin R, Reinhardt T, Vogel G (2011) A description of the nonhydrostatic regional model LM. Part II: physical parameterization, Deutscher Wetterdienst. <http://www.cosmo-model.org/content/model/documentation/core/cosmoPhysParamtr.pdf>. Accessed 25 June 2016
- Dufresne JL et al (2012) Climate change projections using the IPSL-CM5 Earth System Model: from CMIP3 to CMIP5. *Clim Dyn* doi:[10.1007/s00382-012-1636-1](https://doi.org/10.1007/s00382-012-1636-1)
- Dunne JP et al (2012) GFDL's ESM2 global coupled climate-carbon Earth System models. Part I: physical formulation and baseline simulation characteristics. *J Clim* 25:6646–6665
- Dwyer JG, Norris JR, Ruckstuhl C (2010) Do climate models reproduce observed solar dimming and brightening over China and Japan? *J Geophys Res* 115:D00K08. doi:[10.1029/2009JD012945](https://doi.org/10.1029/2009JD012945)
- Ek MB, Mitchell KE, Lin Y, Rogers E, Grunmann P, Koren V, Gayno G, Tarpley JD (2003) Implementation of Noah land surface model advances in the National Centers for Environmental Prediction operational mesoscale Eta model. *J Geophys Res* 003296:2003. doi:[10.1029/2002JD](https://doi.org/10.1029/2002JD)
- Feser F, Rockel B, von Storch H, Winterfeldt J, Zahn M (2011) Regional climate models add value to global model data. *Bull Am Meteorol Soc* 92:1181–1192
- Finger D, Heinrich G, Gobiet A, Bauder A (2012) Projections of future water resources and their uncertainty in a glacierized catchment in the Swiss Alps and the subsequent effects on hydropower production during the 21st century. *Water Resour Res* 48:W02521. doi:[10.1029/2011WR010733](https://doi.org/10.1029/2011WR010733)
- Folini D, Wild M (2011) Aerosol emissions and dimming/brightening in Europe: sensitivity studies with ECHAM5-HAM. *J Geophys Res* 116:D21104. doi:[10.1029/2011JD016227](https://doi.org/10.1029/2011JD016227)
- Fouquart Y, Bonnel B. (1980). Computations of solar heating of the earth's atmosphere: A new parametrization. *Beitr Phys Atmo* 53:35–62
- Gaetani M et al (2014) The near future availability of photovoltaic energy in Europe and Africa in climate-aerosol modelling experiments. *Renew Sust Energy Rev* 38:706–716
- García Díez M, Fernández J, Vautard R (2015) An RCM multiphysics ensemble over Europe: multivariable evaluation to avoid error compensation. *Clim Dyn* 45(11):3141–3156. doi:[10.1007/s00382-015-2529-x](https://doi.org/10.1007/s00382-015-2529-x)
- Gilgen H, Wild M, Ohmura A (1998) Means and trends of shortwave irradiance at the surface estimated from global energy balance archive data. *J Clim* 11(8):2042–2061
- Giorgi F, Bi X (2000) A study of internal variability of a regional climate model. *J Geophys Res* 105:29503–29521
- Giorgi F, Gutowski Jr WJ (2015) Regional Dynamical Downscaling and the CORDEX Initiative. *Annu Rev Environ Resour* 40:467–490
- Giorgi F, Marinucci MR, Visconti G (1990) Use of a limited area model nested in a general circulation model for regional climate simulation over Europe. *J Geophys Res* 95(18):413–418
- Gobiet A, Jacob D, EURO-CORDEX Community (2012) A new generation of regional climate simulations for Europe: the EURO-CORDEX initiative. *Geophys Res Abstracts* 14:EGU2012-8211
- Grell GA, Devenyi D (2002) A generalized approach to parameterizing convection combining ensemble and data assimilation techniques. *Geophys Res Lett* 015311:2002. doi:[10.1029/2002GL](https://doi.org/10.1029/2002GL)
- Hahn CJ, Warren SG (2003) Cloud climatology for land stations worldwide, 1971–1996, NDP-026D. Carbon Dioxide Information Analysis Center, Oak Ridge National Laboratory, Oak Ridge, TN, doi:[10.3334/CDIAC/cli.ndp026d](https://doi.org/10.3334/CDIAC/cli.ndp026d). <http://cdiac.ornl.gov/epubs/ndp/ndp026d/ndp026d.html>
- Haywood JM, Bellouin N, Jones A, Boucher O, Wild M, Shine KP (2011) The roles of aerosol, water vapor and cloud in future global dimming/brightening. *J Geophys Res* 116:D20203. doi:[10.1029/2011JD016000](https://doi.org/10.1029/2011JD016000)
- Hazeleger W et al (2012) EC-Earth V2.2: description and validation of a new seamless earth system prediction model. *Clim Dyn* 39:2611–2629
- Hohenegger C, Vidale PL (2005) Sensitivity of the European climate to aerosol forcing as simulated with a regional climate model. *J Geophys Res* 110:D06201. doi:[10.1029/2004JD005335](https://doi.org/10.1029/2004JD005335)
- Hong SY, Dudhia J, Chen SH (2004) A revised approach to microphysical processes for the bulk parameterization of cloud and precipitation. *Mon Weather Rev* 132:103–120
- Hong SY, Noh Y, Dudhia J (2006) A new vertical diffusion package with an explicit treatment of entrainment processes. *Mon Weather Rev* 134:2318–2341. [http://www.dwd.de/bvbw/generator/DWDWWW/Content/Forschung/FE1/Veroeffentlichungen/Download/LMdocu\\_\\_II\\_\\_physics\\_\\_0509,templateId=raw,property=publicationFile.pdf/LMdocu\\_\\_II\\_\\_physics\\_\\_0509.pdf](http://www.dwd.de/bvbw/generator/DWDWWW/Content/Forschung/FE1/Veroeffentlichungen/Download/LMdocu__II__physics__0509,templateId=raw,property=publicationFile.pdf/LMdocu__II__physics__0509.pdf) Accessed on 20 August 2015
- Iacono MJ, Delamere JS, Mlawer EJ, Shephard MW, Clough SA, Collins WD (2008) Radiative forcing by long-lived greenhouse gases: calculations with the AER radiative transfer models. *J Geophys Res* 113:D13103. doi:[10.1029/2008JD009944](https://doi.org/10.1029/2008JD009944)
- IPCC Climate Change (2013) The physical science basis. In: Stocker TF, Qin D, Plattner GK, Tignor M, Allen SK, Boschung J, Nauels A, Xia Y, Bex V, Midgley PM (eds) Contribution of working group I to the fifth assessment report of the intergovernmental panel on climate change. Cambridge University Press, Cambridge, p 1535. doi:[10.1017/CBO9781107415324](https://doi.org/10.1017/CBO9781107415324)
- Jacob D, Petersen J, Eggert B, Alias A, Christensen OB, Bouwer LM et al (2014) EURO-CORDEX: new high-resolution climate change projections for European impact research. *Reg Environ Change* 14(2):563–578
- Jaeger E, Anders I, Luthi D, Rockel B, Schar C, Seneviratne SI (2008) Analysis of ERA40-driven CLM simulations for Europe. *Meteorol Z* 17(4):349–367
- Jerez S, Montavez JP, Gomez-Navarro JJ, Jimenez PA, Jimenez-Guerrero P, Lorente R, Gonzalez-Rouco JF (2012) The role of the land-surface model for climate change projections over the Iberian Peninsula. *J Geophys Res* 117:D01109
- Jerez S, Montavez JP, Jimenez-Guerrero P, Gomez-Navarro JJ, Lorente-Plazas R, Zorita E (2013) A multi-physics ensemble of present-day climate regional simulations over the Iberian Peninsula. *Clim Dyn* 40(11–12):3023–3046
- Jerez S, Thais F, Tobin I, Wild M, Colette A, Yiou P, Vautard R (2015) The CLMIX model: a tool to create and evaluate spatially-resolved scenarios of photovoltaic and wind power development. *Renew Sustain Energy Rev* 42:1–15. doi:[10.1016/j.rser.2014.09.041](https://doi.org/10.1016/j.rser.2014.09.041)

- Kain JS, Fritsch JM (1990) A one-dimensional entraining/detraining plume model and its application in convective parameterization. *J Atmos Sci* 47:2784–2802
- Kain JS, Fritsch JM (1993) Convective parameterization for mesoscale models: the Kain-Fritsch scheme. The representation of cumulus convection in numerical models. *Meteorol Monogr* 24:165–170
- Katragkou E, García-Díez M, Vautard R, Sobolowski S, Zanis P, Alexandri G, Cardoso RM, Colette A, Fernandez J, Gobiet A, Goergen K, Karacostas T, Knist S, Mayer S, Soares PMM, Pytharoulis I, Tegoulis I, Tsikerdekis A, Jacob D (2015) Regional climate hindcast simulations within EURO-CORDEX: evaluation of a WRF multi-physics ensemble. *Geosci Model Dev* 8:603–618. doi:10.5194/gmd-8-603-2015
- Kinne S, O'Donnel D, Stier P, Kloster S, Zhang K, Schmidt H, Rast S, Giorgetta M, Eck FT, Stevens B (2013) HAC-v1: a new global aerosol climatology for climate studies. *J Adv Model Earth Syst* 5:1–37. doi:10.1002/jame.20035
- Klein SA, Zhang Y, Zelinka MD, Pincus R, Boyle J, Gleckler PJ (2013) Are climate model simulations of clouds improving? An evaluation using the ISCCP simulator. *J Geophys Res Atmos* 118:1329–1342. doi:10.1002/jgrd.50141
- Kothe S, Dobler A, Beck A, Ahrens B (2011) The radiation budget in a regional climate model. *Clim Dyn* 36:1023–1036. doi:10.1007/s00382-009-0733-2
- Kotlarski S, Keuler K, Christensen OB, Colette A, Déqué M, Gobiet A, Goergen K, Jacob D, Lüthi D, van Meijgaard E, Nikulin G, Schär C, Teichmann C, Vautard R, Warrach-Sagi K, Wulfmeyer V (2014) Regional climate modeling on European scales: a joint standard evaluation of the EURO-CORDEX RCM ensemble. *Geosci Model Dev* 7:1297–1333. doi:10.5194/gmd-7-1297-2014
- Kupiainen M, Samuelsson P, Jones C, Jansson C, Willén U, Hansson U, Ullerstig A, Wang S, Döscher R (2011), Rossby Centre regional atmospheric model, RCA4. Rossby Centre Newsletter, June 2011. SMHI, SE-60176 Norrköping, Sweden, <http://www.smhi.se/en/research/research-departments/climate-research-rossby-centre2-552/rossby-centre-regional-atmospheric-model-rca4-1.16562>. Accessed 25 June 2016
- Lamarque JF, Bond T, Eyring V, Granier C, Heil A, Klimont Z, van Vuuren D (2010) Historical (1850–2000) gridded anthropogenic and biomass burning emissions of reactive gases and aerosols: methodology and application. *Atmos Chem Phys* 10:7017–7039
- Lara-Fanego V, Ruiz-Arias JA, Pozo-Vázquez D, Santos-Alamillos FJ, Tovar-Pescador J (2012) Evaluation of the WRF model solar irradiance forecasts in Andalusia (southern Spain). *Sol Energy* 86(8):2200–2218
- Li JLF, Waliser DE, Stephens G, Lee S, L'Ecuyer T, Kato S, Loeb N, Ma HY (2013) Characterizing and understanding radiation budget biases in CMIP3/CMIP5 GCMs, contemporary GCM, and reanalysis. *J Geophys Res Atmos* 118(15):8166–8184. doi:10.1002/jgrd.50378
- Louis JF (1979) A parametric model of vertical eddy fluxes in the atmosphere. *Bound Layer Meteorol* 17:187–202
- Lucas-Picher P, Caya D, de Elía R, Laprise R (2008) Investigation of regional climate models' internal variability with a ten-member ensemble of 10-year simulations over a large domain. *Clim Dyn*. 31:927–940
- Maraun D, Wetterhall F, Ireson AM, Chandler RE, Kendon EJ, Widmann M, Brienen S, Rust HW, Sauter T, Themeßl M, Venema VKC, Chun KP, Goodess CM, Jones RG, Onof C, Vrac M, Thiele-Eich I (2010) Precipitation downscaling under climate change: recent developments to bridge the gap between dynamical models and the end user. *Rev Geophys* 48:RG3003. doi:10.1029/2009RG000314
- Müller C, Robertson RD (2014) Projecting future crop productivity for global economic modeling. *Agric Econ* 45:37–50. doi:10.1111/agec.12088
- Nabat P, Somot S, Mallet M, Sanchez-Lorenzo A, Wild M (2014) Contribution of anthropogenic sulfate aerosols to the changing Euro-Mediterranean climate since 1980. *Geophys Res Lett* 41(15):5605–5611. doi:10.1002/2014GL060798
- Noilhan J, Planton S (1989) A simple parameterization of land surface processes for meteorological models. *Mon Weather Rev* 117:536–549
- Ohmura A, Gilgen H, Wild M (1989) Global Energy Balance Archive, GEBA-World Climate Programme-Water Project A7, Report 1: introduction. Zürcher Geographische Schriften, No.34. Fachvereine Verlag, Zurich, p 62
- Ohmura A, Dutton EG, Forgan B, Frohlich C, Gilgen H, Hegner H, Heimo A, König-Langlo G, McArthur B, Müller G, Philipona R, Pinker R, Whitlock CH, Dehne K, Wild M (1998) Baseline surface radiation network (bsrn/wcrp): new precision radiometry for climate research. *Bull Am Meteorol Soc* 79(10):2115–2136
- Paeth H, Mannig B (2013) On the added value of regional climate modeling in climate change assessment. *Clim Dyn* 41:1057–1066. doi:10.1007/s00382-012-1517-7
- Panagea IS, Tسانis IK, Koutroulis AG, Grillakis MG (2014) Climate change impact on photovoltaic energy output: the case of Greece. *Adv Meteorol* 2014:264506
- Pasicko R, Brankovic C, Simic Z (2012) Assessment of climate change impacts on energy generation from renewable sources in Croatia. *Renew Energy* 46:224–231
- Pessacg NL, Solman SA, Samuelsson P, Sanchez E, Marengo J, Li L, Remedio ARC, da Rocha RP, Mourao C, Jacob D (2014) The surface radiation budget over South America in a set of regional climate models from the CLARIS-LPB project. *Clim Dyn* 43:1221–1239. doi:10.1007/s00382-013-1916-4
- Rasch PJ, Kristjánsson JE (1998) A comparison of the CCM3 model climate using diagnosed and predicted condensate parameterizations. *J Climate* 11:1587–1614
- Remund J, Müller SC (2010) Trends in global radiation between 1950 and 2100. 10th EMS Annual Meeting, 10th European Conference on Applications of Meteorology (ECAM). European Meteorological Society (EMS), Zurich
- Ricard JL, Royer JF (1993) A statistical cloud scheme for use in an AGCM. *Ann Geophys* 11:1095–1115
- Ritter B, Geleyn JF (1992) A comprehensive radiation scheme of numerical weather prediction with potential application to climate simulations. *Mon Weather Rev* 120:303–325
- Rotstayn LD, Jeffrey SJ, Collier MA, Dravitzki SM, Hirst AC, Syktus JJ, Wong KK (2012) Aerosol- and greenhouse gas-induced changes in summer rainfall and circulation in the Australasian region: a study using single-forcing climate simulations. *Atmos Chem Phys* 12:6377–6404
- Ruckstuhl C, Norris JR (2009) How do aerosol histories affect solar “dimming” and “brightening” over Europe? IPCC-AR4 models versus observations. *J Geophys Res* 114:D00D04. doi:10.1029/2008JD011066
- Rummukainen M (2010) State-of-the-art with regional climate models. *Wiley Interdiscip Rev Clim Change* 1(1):82–96
- Samuelsson P, Gollvik S, Ullerstig A (2006) The land-surface scheme of the Rossby Centre regional atmospheric climate model (RCA3). SMHI Rep Met 122
- Samuelsson P, Jones C, Willén U, Ullerstig A, Gollvik S, Hansson U, Jansson C, Kjellström E, Nikulin G and Wyser K (2011) The Rossby Centre Regional Climate Model RCA3: model description and performance. *Tellus* 63 A. doi:10.1111/j.1600-0870.2010.00478.x

- Sass BH, Rontu L, Savijaärvi H, Räisänen P (1994) HIRLAM-2 radiation scheme: documentation and tests. SMHI HIRLAM Technical Report No. 16
- Savijärvi H (1990) A fast radiation scheme for mesoscale model and short-range forecast models. *J Appl Meteorol* 29:437–447
- Schewe J, Heinke J, Gerten D, Haddeland I, Arnell NW, Clark DB, Dankers R, Eisner S, Fekete BM, Colón-González FJ, Gosling SN, Kim H, Liu X, Masaki Y, Portmann FT, Satoh Y, Stacke T, Tang Q, Wada Y, Wisser D, Albrecht T, Frieler K, Piontek F, Warszawski L, Kabat P (2014) Multi-model assessment of water scarcity under climate change. *PNAS* 111(9):3245–3250. doi:10.1073/pnas.1222460110
- Seneviratne SI, Corti T, Davin EL, Hirschi M, Jaeger EB, Lehner I, Teuling AJ (2010) Investigating soil moisture–climate interactions in a changing climate: a review. *Earth Sci Rev* 99(3):125–161
- Skamarock WC, Klemp JB, Dudhia J, Gill DO, Barker DM, Duda MG, Huang X-Y, Wang W, Powers JG (2008) A description of the advanced research WRF Version 3, NCAR/TN-475+STR, NCAR Technical Note, June 2008
- Stanhill G, Cohen S (2001) Global dimming: a review of the evidence for a widespread and significant reduction in global radiation with discussion of its probable causes and possible agricultural consequences. *Agric For Meteorol* 107(4):255–278
- Szentimrey T (2003) Multiple analysis of series for homogenization (MASH); Verification procedure for homogenized time series. In: Fourth seminar for homogenization and quality control in climatological databases, WMO, Budapest, 56:193–201
- Tanré D, Geleyn J, Slingo J (1984) First results of the introduction of an advanced aerosol–radiation interaction in ECMWF low resolution global model. In: Gerber H, Deepak A (eds) *Aerosols and their climatic effects*, A. Deepak, Hampton, pp. 133–177
- Taylor KE, Stouffer RJ, Meehl GA (2012) An overview of Cmp5 and the experiment design. *Bull Am Meteorol Soc* 93(4):485–498
- Tegen I, Hollrig P, Chin M, Fung I, Jacob D, Penner J (1997) Contribution of different aerosol species to the global aerosol extinction optical thickness: estimates from model results. *J Geophys Res* 102(23 895–23):915
- Tian T, Boberg F, Christensen OB, Christensen JH, She J, Vihma T (2013) Resolved complex coastlines and land–sea contrasts in a high-resolution regional climate model: a comparative study using prescribed and modelled SSTs. *Tellus A* 65: 19951. doi:10.3402/tellusa.v65i0.19951
- Tiedtke M (1989) A comprehensive mass flux scheme for cumulus parameterization in large-scale models. *Mon Weather Rev* 117:1779–1799
- Tjiputra JF et al (2013) Evaluation of the carbon cycle components in the Norwegian Earth System Model (NorESM). *Geophys Model Dev* 6:301–325
- Torma CS, Giorgi F, Coppola E (2015) Added value of regional climate modeling over areas characterized by complex terrain—Precipitation over the Alps. *J Geophys Res Atmos* 120:3957–3972. doi:10.1002/2014JD022781
- Troen I, Mahrt L (1986). A simple model of the atmosphere boundary layer; sensitivity to surface evaporation. *Bound Layer Meteorol* 37:129–148.
- Turco M, Sanna A, Herrera S, Llasat MC, Gutiérrez JM (2013) Large biases and inconsistent climate change signals in ENSEMBLES regional projections. *Clim Change* 120:859–869
- Turnock ST, Spracklen DV, Carslaw KS, Mann GW, Woodhouse MT, Forster PM, Haywood J, Johnson CE, Dalvi M, Bellouin N, Sanchez-Lorenzo A (2015) Modelled and observed changes in aerosols and surface solar radiation over Europe between 1960 and 2009. *Atmos Chem Phys Discuss* 15:13457–13513
- Vannitsem S, Chomé F (2005) One-way nested regional climate simulations and domain size. *J Clim* 18:229–233
- Vautard R, Gobiet A, Jacob D, Belda M, Colette A, Déqué M et al (2013) The simulation of European heat waves from an ensemble of regional climate models within the EURO-CORDEX project. *Clim Dyn* 41:2555–2575. doi:10.1007/s00382-013-1714-z
- Vezzoli R, Mercogliano P, Pecora S, Zollo AL, Cacciamani C (2015) Hydrological simulation of Po River (North Italy) discharge under climate change scenarios using the RCM COSMO-CLM. *Sci Total Environ* 521–522:346–358
- Voldoire A, Sanchez-Gomez E, Salas y Méliá D, Decharme B, Cassou C, Sénési S, Valcke S, Beau I, Alias A, Chevallier M, Déqué M, Deshayes J, Douville H, Fernandez E, Madec G, Maiconnave E, Moine M-P, Planton S, Saint-Martin D, Szopa S, Tyteca S, Alkama R, Belamari S, Braun A, Coquart L, Chauvin F (2013) The CNRM-CM5.1 global climate model: description and basic evaluation. *Clim Dyn* 40(9–10):2091–2121
- von Salzen K et al (2013) The Canadian Fourth Generation Atmospheric Global Climate Model (CanAM4). Part I: representation of physical processes. *Atmos Ocean* 51:104–125
- Watanabe M et al (2010) Improved climate simulation by MIROC5: Mean states, variability, and climate sensitivity. *J Clim* 23:6312–6335
- Wilcox LJ, Highwood EJ, Dunstone NJ (2013) The influence of anthropogenic aerosol on multi-decadal variations of historical global climate. *Environ Res Lett*. doi:10.1088/1748-9326/8/2/024033
- Wild M (2009) Global dimming and brightening: A review. *J Geophys Res* 114:D00D16. doi:10.1029/2008JDO11470
- Wild M, Schmucki E (2011) Assessment of global dimming and brightening in IPCC-AR4/CMIP3 models and ERA40. *Clim Dyn* 37(7):1671–1688. doi:10.1007/s00382-010-0939-3
- Wild M, Ohmura A, Gilgen H, Roeckner E (1995) Regional climate simulation with a high resolution GCM: surface radiative fluxes. *Clim Dyn* 11:469–486
- Wild M, Dümenil L, Schulz JP (1996) Regional climate simulation with a high resolution GCM: surface hydrology. *Clim Dyn* 12:755–774
- Wild M, Ohmura A, Cubasch U (1997) GCM simulated surface energy fluxes in climate change experiments. *J Clim* 10:3093–3110
- Wild M et al (2005) From dimming to brightening: decadal changes in surface solar radiation. *Science* 308:847–850. doi:10.1126/science.1103215
- Wild M, Folini D, Schär C, Loeb N, Dutton EG, König-Langlo G (2013) The global energy balance from a surface perspective. *Clim Dyn* 40:3107–3134. doi:10.1007/s00382-012-1569-8
- Wild M, Folini D, Henschel F, Fischer N, Müller B (2015a) Projections of long-term changes in solar radiation based on CMIP5 climate models and their influence on energy yields of photovoltaic systems. *Sol Energy* 116:12–24
- Wild M, Folini D, Hakuba MZ, Schär C, Seneviratne SI, Kato S, Rutan D, Ammann C, Wood EF, König-Langlo G (2015b) The energy balance over land and oceans: an assessment based on direct observations and CMIP5 climate models. *Clim Dyn* 44(11–12):3393–3429. doi:10.1007/s00382-014-2430-z
- Xie SP, Deser C, Vecchi GA, Collins M, Delworth TL, Hall A, Hawkins E, Johnson NC, Cassou C, Giannini A, Watanabe M (2015) Towards predictive understanding of regional climate change. *Nat Clim Change* 5:921–930
- Zhang MH et al (2005) Comparing clouds and their seasonal variations in 10 atmospheric general circulation models with satellite measurements. *J Geophys Res* 110:D15S02. doi:10.1029/2004JD005021

- Zubler EM, Folini D, Lohmann U, Lüthi D, Schär C, Wild M (2011a) Simulation of dimming and brightening in Europe from 1958 to 2001 using a regional climate model. *J Geophys Res* 116:D18205. doi:[10.1029/2010JD015396](https://doi.org/10.1029/2010JD015396)
- Zubler EM, Folini D, Lohmann U, Lüthi D, Muhlbauer A, Pousse-Nottelmann S, Schär C, Wild M (2011b) Implementation and evaluation of aerosol and cloud microphysics in a regional climate model. *J Geophys Res* 116:D02211. doi:[10.1029/2010JD014572](https://doi.org/10.1029/2010JD014572)
- Zubler EM, Lohmann U, Lüthi D, Schär C (2011c) Intercomparison of aerosol climatologies for use in a regional climate model over Europe. *Geophys Res Lett* 38:L15705. doi:[10.1029/2011GL048081](https://doi.org/10.1029/2011GL048081)